Role of S4 Segments and the Leucine Heptad Motif in the Activation of an L-Type Calcium Channel

J. García,* J. Nakai,# K. Imoto,# and K. G. Beam*
*Departments of Physiology and Anatomy and Neurobiology, Colorado State University, Fort Collins, Colorado 80523 USA, and #Department of Information Physiology, National Institute for Physiological Sciences, Okazaki 444, Japan

ABSTRACT Basic residues in the S4 segments of voltage-dependent channels and leucines within the heptad repeat motif in the S4-S5 region of *Shaker* potassium channels have been shown to have important influences on activation. Here we have compared the relative importance for activation of S4 arginines (mutated to neutral or negative residues) in each of the four repeats of a chimeric L-type calcium channel. Significant effects on midpoint potential and time constant of activation were produced by mutations in repeats I and III but not in repeats II and IV. Leucine or isoleucine mutations in repeats I and III had the same effect on the voltage dependence of calcium channel activation as the mutations at equivalent positions in the *Shaker* channel, indicating that the heptad motif plays a fundamental role in channel activation.

INTRODUCTION

A common characteristic among voltage-dependent channels is that every third residue in the putative transmembrane segment S4 is positively charged (arginine or lysine) (Noda et al., 1986; Tanabe et al., 1987; Tempel et al., 1987; Schwarz et al., 1988; Mori et al., 1991), and the S4 segment has thus been proposed to be important in voltage sensing. Supporting evidence has come from studies in which positively charged S4 residues were substituted with other residues in potassium channels (Papazian et al., 1991; Liman et al., 1991; Logothetis et al., 1992; Tytgat et al., 1993), in repeats I and II of the rat brain II sodium channel (Stühmer et al., 1989), and in repeats I-IV of the human heart sodium channel (Chen et al., 1996). These substitutions resulted in changes of the voltage dependence of activation (midpoint voltage and steepness). Mutations in the S4 segments have not been examined at all in calcium channels, which are like sodium channels in having four homologous but nonidentical repeats.

Recent evidence is consistent with outward movement of the S4 segment during activation of the *Shaker* potassium channel (Larsson et al., 1996) and of the IVS4 segment during inactivation of the human skeletal muscle sodium channel (Yang et al., 1996). However, the deduced region of S4 movement was much different, which may reflect the difference in channel structure (homotetramer versus four nonidentical repeats) or physiological process studied (activation versus inactivation). In this paper we systematically examined the contribution of charged residues in the S4 segments of each of the repeats to activation of a chimeric calcium channel, SkC15. Single charged residues (arginine) were exchanged for neutral (glutamine) or negative (glutamate) residues at corresponding positions in the S4 segments of repeats I–IV. Most of the mutations caused a decrease in the apparent gating charge, indicating that the channel had a reduced sensitivity to changes in membrane potential. S4 mutations in repeats I and III, but not in II or IV, significantly affected the midpoint potential of activation. All of the mutants in the S4 segment of repeats I and III caused a change in the time constant of activation of the current. These results suggest that repeats I and III are especially important for activation of the calcium channel.

The leucine heptad motif in the *Shaker* potassium channel consists of five leucines, arrayed with a leucine at every seventh residue and spanning the distance from the end of the S4 segment to the beginning of the S5 segment. Conservative substitutions of valine for leucine in the heptad motif had significant effects on the voltage dependence of *Shaker* potassium channels (McCormack et al., 1991; Lopez et al., 1991), affecting both the steepness and midpoint potential of activation to a similar or greater extent than charge-reducing mutations in the S4 segment. Similarly, the L860F mutation in repeat II of the rat brain IIa sodium channel dramatically alters its gating properties (Auld et al., 1990), including a depolarization shift, as seen for the corresponding *Shaker* L/V mutation. Besides being important for activation, the S4-S5 region in the *Shaker* potassium channel is also involved in N-type inactivation (Isacoff et al., 1991). It has recently been reported that the residue at position 391 is especially important for electrostatic and stearic interactions between this region and the inactivation ball (Holmgren et al., 1996).

The heptad motif region is conserved to a varying extent among the voltage-gated channels. We examined the significance of this region in repeats I and III of the SkC15 calcium channel, replacing leucine or isoleucine with valine. In both repeats I and III, mutation of the leucine closer to the S4 segment caused a positive shift of the half-activation potential, whereas substitution of the leucine/isoleucine closer to S5 caused a negative shift. These shifts

Received for publication 15 November 1996 and in final form 3 March 1997.

Address reprint requests to Dr. Jesús García, Department of Physiology and Biophysics (M/C 902), University of Illinois at Chicago, 900 South Ashland Avenue, Chicago, IL 60607. Tel.: 312-355-0260. Fax: 312-355-0470; E-mail: garmar@uic.edu.

0006-3495/97/06/2515/09 $2.00

were similar in magnitude to those of the S4 mutants. Moreover, the shifts caused by the heptad repeat mutations were in the same direction as the corresponding mutations in the *Shaker* channel. Thus the heptad repeat motif seems to play a similarly fundamental role in the activation of voltage-dependent potassium, sodium, and calcium channels.

EXPERIMENTAL PROCEDURES

Mutagenesis and sequencing

Single amino acid substitutions using the polymerase chain reaction (PCR) were performed for mutants R171E, R653Q, R656Q, R653Q-R656Q, R1031Q, R1034Q, L1045V, and I1059V. Two PCR fragments were produced in separate but parallel reactions. Each fragment was generated with a constant amplification primer (specific for each repeat) and a mutation primer; the final mutated fragments were obtained by amplifying the two complementary PCR products in a third reaction (Silver et al., 1995). The reaction conditions for each tube consisted of 0.5 μg template DNA (SkC15), 100 pmol of each primer, 400 μM each deoxyribonuclease triphosphate (dNTP) (Pharmacia Biotech, Alameda, CA), 5 units *hot tub* DNA polymerase (Amersham, Arlington Heights, IL), 10 μl polymerase buffer (10×), and sterilized distilled water suficient to bring the total volume to 100 μl. Thirty-six amplification cycles were performed with the thermal cycler (Perkin-Elmer, Norwalk, CT); cycle 1, 94°C for 4 min, 58°C for 1 min, 72°C for 2 min; cycles 2–36, 94°C for 30 s, 58°C for 1 min, 72°C for 2 min. After the last cycle an additional 5-min extension period at 72°C was used. PCR products were subcloned in pBluescript (Stratagene, CA). The rest of the mutants were constructed using site-directed mutagenesis following the procedure described by Sayers and Eckstein (1989). The entire PCR fragment was sequenced by the chain termination method (Sanger et al., 1977), using synthetic oligonucleotides as primers.

Expression of mutants

Complementary DNA encoding each mutant was injected into the nuclei of dysgenic myotubes in culture. Myotubes were injected on the seventh day after initial plating and were examined 2–3 days later. Myotubes expressing the mutants were identified by contractions in response to electrical stimuli. cDNA for mutant R653Q was coinjected with cDNA encoding the α subunit of the human surface antigen CD8, provided by Dr. Brian Seed (Massachusetts General Hospital, Boston) (see Jurman et al., 1994). These myotubes were later identified with polystyrene beads coated with CD8 antibody (1.4×10^8 beads/ml; Dynal, New York).

Electrophysiological recordings

Calcium currents were recorded using the whole-cell configuration of the patch-clamp technique (Hamill et al., 1981). Analog compensation was used to reduce the effective series resistance to <1 MΩ. The linear cell capacitance was charged with a time constant of <1 ms. Cell capacitance was determined by integration of a control current trace obtained with a 30-mV hyperpolarizing pulse from the holding potential. This capacitance was used to calculate the density of calcium currents (pA/pF). A two time-constant analog circuit was used to cancel the bulk of the linear capacitative current during a series of test pulses. Voltage clamp commands were rounded at 1 kHz with a Bessel low-pass filter. Linear capacitative and resistive current were subtracted from test currents. T-type calcium current was inactivated by applying a 1-s prepulse to −30 mV. The prepulse was followed by a pedestal to −50 mV, from which the test pulses (15 or 200 ms) were applied (Adams et al., 1990). The holding potential was −80 mV.

Maximum amplitude of the calcium current during the 15-ms pulses was measured, plotted as a function of voltage, and used to calculate the normalized conductance (G) versus voltage relationship (García et al., 1994). Although activation was not complete for the 15-ms test pulses, the resulting G-V curve should be identical to that obtained with long-duration test pulses if τ_{act} were voltage-independent. In fact, τ_{act} for skeletal-type calcium channels does not vary greatly with voltage (Dirksen and Beam, 1996). Moreover, the effects of mutations on the G-V parameters were not simply a secondary result of changes in τ_{act}, because the changes in G-V parameters and τ_{act} were uncorrelated (see Table 1). Values for $V_{1/2}$ and z_g were obtained by fitting the following equation to the normalized conductance:

$$G/G_{max} = 1/[1 + \exp\{(V_{1/2} - V)/k\}] \quad (1)$$

z_g was calculated from RT/Fk. R, T, and F have the usual thermodynamic meaning, and RT/F equals 25.5 mV at the temperature of our experiments.

Patch pipettes were made from borosilicate glass and had resistances of 1.6–2.0 MΩ when filled with "internal solution," which contained (in mM): 145 Cs-aspartate, 10 HEPES, 5 Mg_2Cl, and 10 Cs_2EGTA. The external solution contained (in mM): 145 tetraethylammonium-Cl, 10 HEPES, 10 $CaCl_2$, and 0.003 tetrodotoxin. The pH of the internal and external solutions was adjusted to 7.4 with CsOH. Experiments were conducted at room temperature (22–24°C).

RESULTS

Targeted residues in the S4 region and the heptad repeat motif

For our experiments, we used the chimeric dihydropyridine (DHP)-sensitive calcium channel SkC15 (Fig. 1, *top*) because it expresses at high level after injection of its cDNA into dysgenic myotubes (Tanabe et al., 1991). Furthermore, SkC15 produces slowly activating current distinct from the small calcium current endogenous to dysgenic myotubes (Adams and Beam, 1989). Fig. 1 illustrates the alignment of the S4 segments and heptad motif regions of the four repeats of the skeletal and cardiac L-type calcium channels with those of the BI calcium channel (A-type), sodium channel, and *Shaker* potassium channel. The *Shaker* sequence is shown only in the alignment of repeat IV, because this channel functions as a homotetramer (Tempel et al., 1987; MacKinnon, 1991). The charged (basic) residues arginine (R) and lysine (K), which occur at every third position of S4, are indicated by plus signs. If S4 segments participate in voltage sensing, reducing the S4 charge should alter the voltage dependence of activation. To compare the relative importance of S4 segments in each of the four repeats, arginines were mutated to the neutral glutamine (Q) at equivalent positions in each of the repeats, as indicated by the vertical boxes.

The heptad motif, which extends from the end of S4 to the beginning of S5 of the *Shaker* potassium channel, consists of a series of five leucines (L) repeated every seventh amino acid (see Fig. 1). The positions corresponding to these leucines are indicated by asterisks. In *Shaker* potassium channels, it has been demonstrated that L → valine (V) mutations (McCormack et al., 1991) or L → alanine (A) mutations (Lopez et al., 1991) cause alterations in voltage dependence of equal or greater magnitude than mutations of the charged S4 residues. We substituted valine for the second and fourth residues (L/I) of the heptad motif in repeats I and III, because the comparable mutations were shown to cause large, oppositely directed voltage shifts in

TABLE 1 Activation parameters and time constant of activation of the calcium current

	$V_{1/2}$ (mV)	k (mV)	z_g	n	τ_{act} (ms)	n
SkC15	12.0 ± 0.8	4.9 ± 0.2	5.4 ± 0.3	22	10.9 ± 0.4	20
Repeat I						
R168Q	13.2 ± 1.6	6.3 ± 0.3	4.1 ± 0.2	5	18.4 ± 1.2	5
R171Q	22.2 ± 1.5	6.1 ± 0.3	4.2 ± 0.2	5	15.7 ± 1.2	5
R171E	28.1 ± 1.1	8.7 ± 0.3	3.0 ± 0.1	17	7.3 ± 0.8	11
L182V	18.1 ± 1.7	8.5 ± 0.3	3.0 ± 0.1	6	16.5 ± 0.7	6
L196V	5.4 ± 0.5	5.7 ± 0.4	4.6 ± 0.3	8	10.5 ± 0.9	7
Repeat II						
R656Q	12.6 ± 1.0	5.5 ± 0.2	4.7 ± 0.2	13	12.4 ± 1.0	10
R653Q-R656Q	12.7 ± 1.6	5.8 ± 0.3	4.6 ± 0.2	13	11.0 ± 0.5	11
Repeat III						
R1031Q	16.3 ± 1.4	6.3 ± 0.2	4.1 ± 0.1	9	16.6 ± 1.1	8
R1034Q	7.7 ± 1.5	6.2 ± 0.3	4.2 ± 0.2	7	14.0 ± 0.9	10
L1045V	20.1 ± 1.3	5.9 ± 0.2	4.4 ± 0.1	10	11.0 ± 0.8	9
I1059V	3.6 ± 1.2	4.9 ± 0.3	5.4 ± 0.4	10	9.2 ± 0.7	8
Repeat IV						
R1362Q	12.5 ± 0.7	6.1 ± 0.2	4.2 ± 0.1	12	11.5 ± 0.7	11
R1365Q	13.8 ± 0.8	5.2 ± 0.1	5.0 ± 0.1	12	11.0 ± 0.4	12
Shaker wild-type	1 ± 5	3.7 ± 0.05	6.8	15		
V2	69 ± 7	11.0 ± 0.9	2.3	7		
V4	−22 ± 3	3.6 ± 0.5	7.0	5		

Activation parameters for the parental calcium channel, SkC15, and for its S4 and heptad motif mutants. Values are mean ± SEM. $V_{1/2}$ and k were obtained by fitting the normalized conductance versus voltage for each cell according to Eq. 1 as described in the Experimental Procedures. z_g is the apparent gating charge obtained by dividing 25.5 (*RT/F* at 23°C) by k. The time constant of activation (τ_{act}) was determined as described in the legend to Fig. 5. The current restored by mutant R653Q was too small to be analyzed accurately; its average amplitude (in myotubes coinjected with CD8) was 0.36 ± 0.23 pA/pF (n = 11). Underlining indicates statistically significant differences from values for SkC15, with $p < 0.05$ for $V_{1/2}$, k, and z_g or $p < 0.001$ for τ_{act}. Data in the bottom three rows are for wild-type and leucine-to-valine (V2 and V4) mutants of the *Shaker* potassium channel and are from McCormack et al. (1991). V2 corresponds to the SkC15 substitutions L182V in repeat I and L1045V in repeat III, and V4 corresponds to L196V in repeat I and I1059V in repeat III (cf. Fig. 1). The k values for the *Shaker* potassium channel were obtained from inactivation curves and $V_{1/2}$ from conductance-versus-voltage curves.

activation of the *Shaker* channel (McCormack et al., 1991). We chose repeat I because it is responsible for the slow activation of the SkC15 calcium current (Tanabe et al., 1991), and repeat III because it contains the least well conserved heptad motif.

Calcium currents were recorded after injection of cDNA encoding SkC15 and its mutants into nuclei of dysgenic myotubes. Representative currents, elicited by 200-ms test pulses, are illustrated in Fig. 2 for SkC15 and the mutants producing the largest (I1059V) and smallest (R171E) measureable currents. Because some of the mutants produced very large current, the steepness and voltage dependence of activation were measured with 15-ms test pulses to reduce current amplitude and thus improve voltage control. The use of short pulses should have only a modest effect on the shape of the conductance-voltage curves, because the activation rate of skeletal-like calcium channels is only weakly voltage dependent (Dirksen and Beam, 1996). With 15-ms test pulses, the average (±SEM) maximum current ranged in amplitude from 3.5 ± 0.6 pA/pF (n = 17) for R171E to 32.6 ± 6.3 pA/pF (n = 10) for I1059V, compared to 17.4 ± 1.8 pA/pF (n = 22) for SkC15. The mutant R653Q restored a current too small to be studied accurately and often did not restore measureable current. To identify the myotubes that had been injected with R653Q, cDNA encoding this mutant was coinjected with cDNA encoding the α-subunit of the human CD8 antigen (kindly provided by Dr. Brian Seed, Massachusetts General Hospital, Boston). These myotubes were subsequently identified with polystyrene microspheres precoated with antibody to CD8 (Jurman et al., 1994). The current recorded from these myotubes averaged 0.36 ± 0.23 pA/pF (n = 11). The amplitude of the current in R653Q-injected cells was not increased by changing the holding potential to more negative values (< −80 mV) or by applying pulses that were longer or more positive. This residue seems to have a similarly critical role in the RCK1 potassium channel, because substitution of R298 (which corresponds to R653 in SkC15) by glutamine, isoleucine, leucine, or asparagine resulted in a lack of expression of current (Liman et al., 1991). Interestingly, an appreciable calcium current (11.4 ± 1.8 pA/pF) was restored by the double SkC15 mutant R653Q-R656Q. This result suggests that a structural disruption produced by the charge-reducing mutation R653Q is at least partially compensated for by the

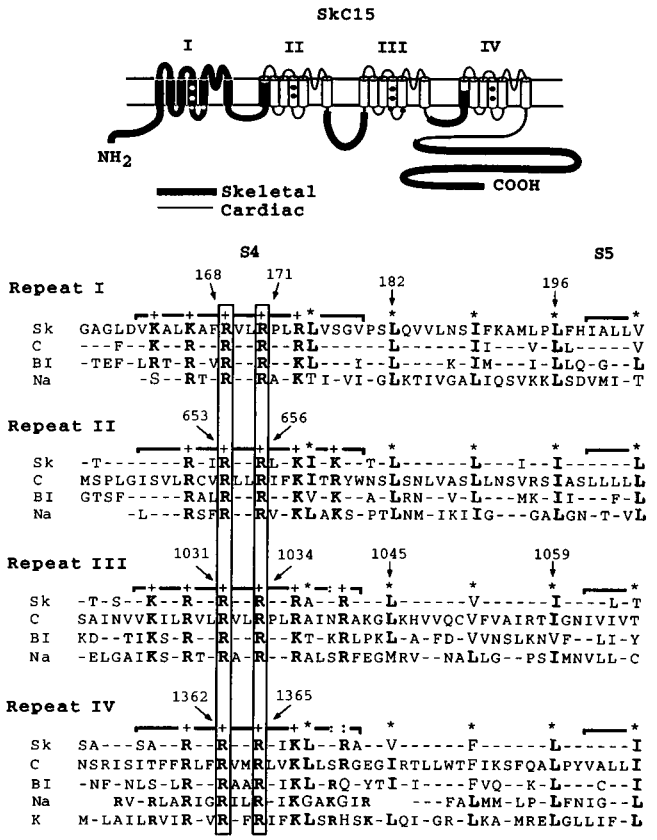

FIGURE 1 Structure of the SkC15 chimeric calcium channel and sequence alignment of the S4 and heptad motif regions of voltage dependent channels. (*Top*) Schematic representation of SkC15, in which repeat I, the amino- and carboxyl-terminals, and the putative cytoplasmic loops have skeletal muscle sequence and the rest of the protein has cardiac sequence (Tanabe et al., 1991). Repeats are numbered above the putative transmembrane segments, and circles indicate the locations of residues that were mutated. (*Bottom*) Alignment for five voltage-dependent channels of the S4 segments (*delimited by brackets*), S4-S5 linkers, and the beginning of the S5 segments (*partial brackets*). Sk, skeletal muscle α_1 subunit (Tanabe et al., 1987, 1988); C, cardiac muscle α_1 subunit (Mikami et al., 1989); BI, brain calcium channel (Mori et al., 1991); Na, brain sodium channel II (Noda et al., 1986); K, *Shaker* potassium channel (Tempel et al., 1987), which is shown aligned only with repeat IV. Plus signs mark the positively charged amino acids within the S4 segments, and asterisks indicate the positions corresponding to the leucine residues of the *Shaker* channel heptad motif. Residues that were mutated are enclosed in vertical boxes and indicated by the numbered residues, which refer to the skeletal sequence in repeat I and to the cardiac sequence in repeats II to IV. Dashes indicate identity to either the skeletal sequence (repeat I) or cardiac sequence (repeats II–IV); blanks indicate gaps introduced to allow alignment of the Na channel sequence with the other channels. The first amino acid shown in the sequence for Sk, C, BI, and Na corresponds, respectively, to residues 156, 258, 186, and 213 for repeat I; 519, 641, 574, and 845 for repeat II; 892, 1019, 1346, and 1297 for repeat III; and 1227, 1350, 1661, and 1626 for repeat IV. The sequence for K starts with amino acid 356.

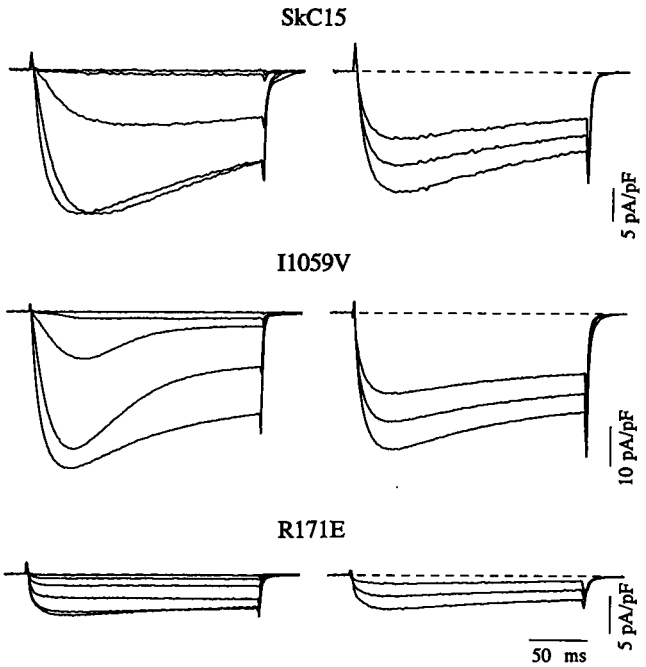

FIGURE 2 Calcium currents in dysgenic myotubes expressing SkC15 or its mutants I1059V and R171E. Currents were evoked by 200-ms test pulses, which ranged (in 10-mV increments), for SkC15, from −20 to 20 mV (*left*) and 30 to 50 mV (*right*); for I1059V, from −30 to 10 mV (*left*) and from 20 to 40 mV (*right*); for R171E, from −10 to 40 mV (*left*) and from 50 to 70 mV (*right*). On average, I1059V restored the largest calcium current, whereas R171E restored the smallest current.

additional, charge-reducing mutation R656Q. The mechanism of this compensation seems to differ from that described by Papazian et al. (1995), in which nonfunctional S4 mutants of the *Shaker* K channel could be rescued by mutations that compensated for the change in net charge.

Effect of the mutations on the voltage dependence of activation

The voltage dependence of activation for SkC15 and its mutants was analyzed by measuring the amplitude of the current in response to test pulses to potentials ranging from −40 to 90 mV (15-ms duration). The calcium current-versus-voltage relationship for each cell was converted into a conductance-voltage (*G-V*) relationship based on the assumption of an ohmic channel (Dirksen and Beam, 1995) and the extrapolated reversal potential. The *G-V* relationship was then fitted with a Boltzmann function to determine the midpoint potential ($V_{1/2}$) and apparent gating charge (z_g). Fig. 3 illustrates normalized conductance-voltage curves (*top*) for SkC15, R171Q, and I1059V. Average $V_{1/2}$ values (±SEM) for these and the other constructs studied are shown in the middle and bottom panels of Fig. 3, with dashed lines representing ±SD for the SkC15 values. With the exception of R168Q, all of the mutations in repeats I and III that reduced the S4 charge by 1 significantly shifted $V_{1/2}$ (*middle panel*, $p < 0.05$). Mutations in repeats II and IV that reduced S4 charge by 1 did not have a significant effect (see also Table 1). As a stronger test of the importance of S4 in repeat II (IIS4), we constructed and examined the mutant (R653Q-R656Q), which reduces the S4 charge by 2. This double mutation also had no effect on $V_{1/2}$. By contrast, a double charge reduction in IS4 (R171E) had a much larger

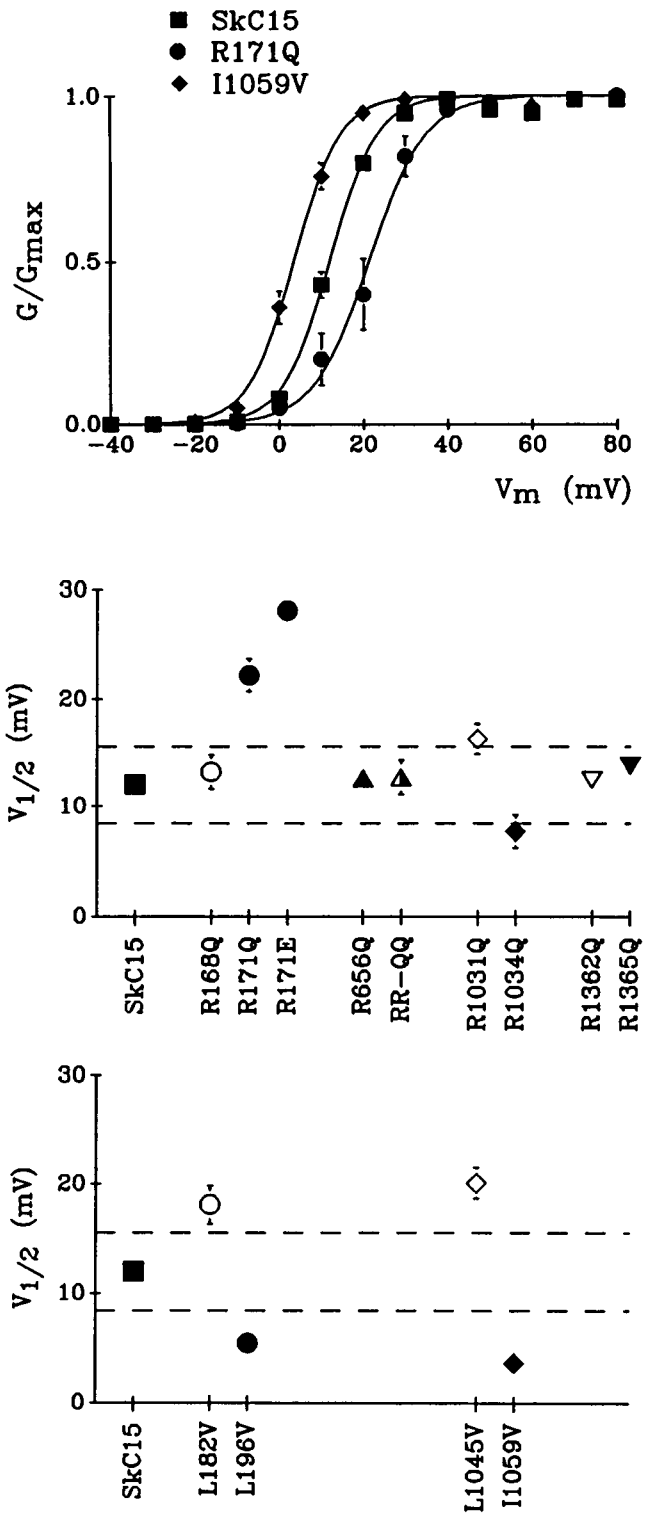

FIGURE 3 Effect of calcium channel mutations on the midpoint potential of activation ($V_{1/2}$). (*Top*) Activation of conductance as a function of test potential for the parental SkC15 calcium channel (*squares*); the mutant R171Q (*circles*), which caused a positive shift in activation; and the mutant I1059V (*diamonds*), which caused a negative shift. Here and in subsequent figures, the error bars represent ± SEM. The smooth curves are least-squares fits of Eq. 1 to the experimental data, with parameters given in Table 1. (*Middle*) Average values of $V_{1/2}$ for the S4 mutants of the SkC15 calcium channel. Circles, triangles, diamonds and inverted triangles are used for mutants in repeats I, II, III and IV, respectively, with open symbols for mutations closer to the amino terminus and filled symbols for mutations closer to the carboxyl terminus. RR-QQ indicates the mutant R653Q-R656Q and is represented by a half-filled triangle. Here and in subsequent figures, the mean value for SkC15 is given by the solid square, with dashed lines representing ± SD. Only the mutations in repeats I and III significantly affected $V_{1/2}$. (*Bottom*) Average values of $V_{1/2}$ for the heptad motif mutants of SkC15. Note that both mutations closer to S4 (*open symbols*) caused a depolarizing shift of $V_{1/2}$, whereas both mutations closer to S5 (*filled symbols*) caused a hyperpolarizing shift.

effect than a single charge reduction (R171Q). There was no correlation between the direction or magnitude of the shift and the location of the mutation (*open symbols* indicate residues closer to the N-terminal end of S4, and *filled symbols* indicate residues closer to the C-terminal end). Similar results were obtained with potassium channels (Papazian et al., 1991; Liman et al., 1991). However, with the rat brain sodium channel (Stühmer et al., 1989), neutralization of charged residues nearer the C-terminal end of S4 segment tended to cause a positive shift, whereas neutralization nearer the N-terminal end caused negative shifts.

Mutations in the heptad motif had effects on $V_{1/2}$ that were more consistent than those of the mutations in the S4 basic residues. The replacement of the leucine closer to the S4 segment in both repeat I (L182V) and repeat III (L1045V) caused a depolarizing shift in activation (Fig. 3, *lower panel*). On the other hand, the mutations closer to S5 in repeat I (L196V) and repeat III (I1059V) both caused a hyperpolarizing shift in activation. The magnitude of the shifts was larger for the mutations in repeat III. The direction of the shifts (depolarizing or hyperpolarizing) for both repeats I and III of the calcium channel was the same as for the leucine mutations at equivalent postions of the potassium channel (McCormack et al., 1991; Lopez et al., 1991).

Except for R1365Q, all of the mutations reducing S4 charge by 1 caused a decrease in z_g (Fig. 4, *middle panel*; Table 1). A decrease in z_g is what one would predict if the basic residues of S4 constitute the gating charge that senses voltage. However, z_g was also reduced by three of the four charge-conserving mutations (L182V, L196V, and L1045V) in the heptad motifs. This reduction could be interpreted as a decreased movement of the voltage sensor, a possibility that also exists for the S4 mutations. Another mechanism that would alter z_g is a large voltage shift in the movement of the voltage sensor in one repeat relative to that of the other voltage sensors. However, for neither the S4 nor the heptad motif mutations was there a correlation between the absolute magnitudes of the shift in $V_{1/2}$ and the decrease in z_g. Similarly, heptad mutations in the *Shaker* channel also do not appear to affect z_g and $V_{1/2}$ in a correlated manner (McCormack et al., 1991). A change in z_g could also result from changes in the magnitude, but not the voltage dependence, of rate constants in a multistep, sequential activation scheme (Sigworth, 1993).

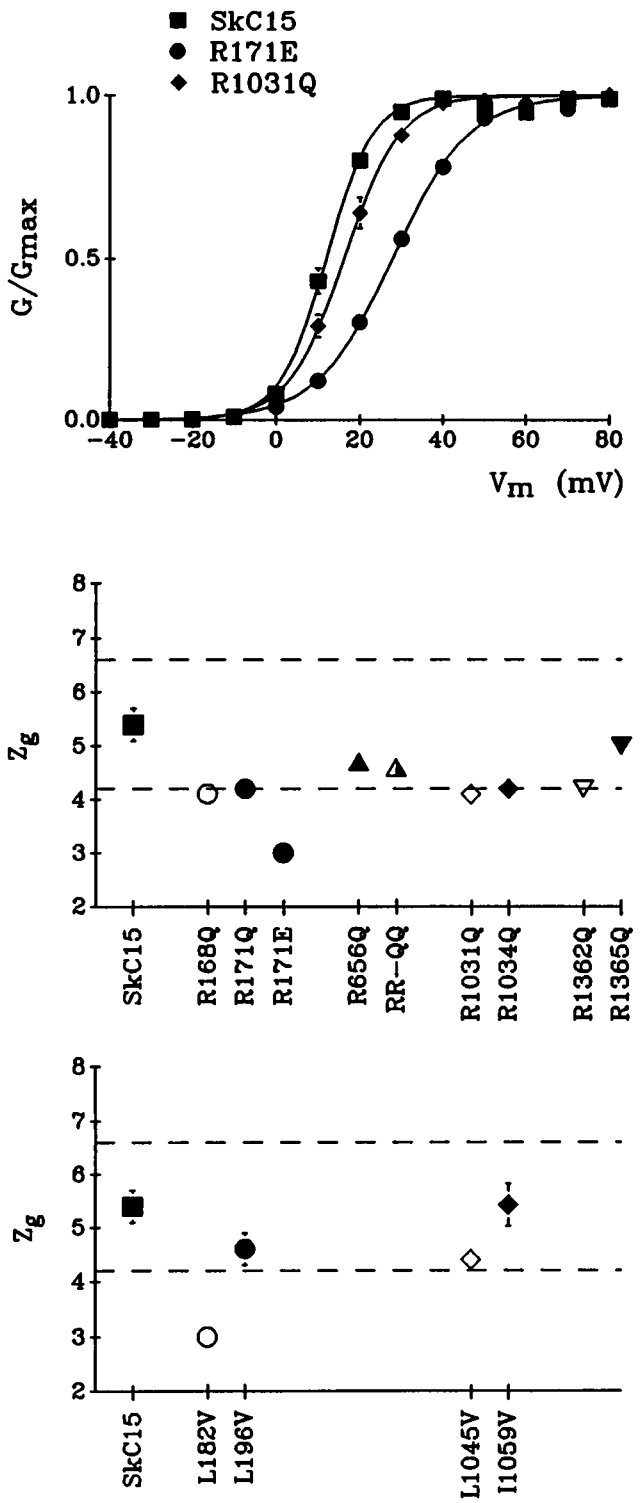

FIGURE 4 Effect of calcium channel mutations on the effective gating charge, z_g. (*Top*) Conductance as a function of test potential for SkC15 (*squares*); for R171E, which caused a large decrease in the steepness of activation; and for R1031Q (*circles*), which caused a relatively small decrease. Smooth curves were calculted according to Eq. 1, with parameter values given in Table 1. Average values of z_g for the S4 and heptad motif mutants are plotted in the middle and bottom panels, respectively. With the exception of I1059V and R1365Q, the S4 and heptad motif mutations all caused a statistically significant decrease in z_g.

Activation rate is also modified by the mutations

In addition to characterizing the effects of the mutations on voltage dependence of activation, we also analyzed their effects on activation rate. For this purpose, it was necessary to use 200-ms test pulses so that activation of current was complete. Because activation rate is only weakly voltage dependent for test potentials greater than or equal to the test potential eliciting peak current (Dirksen and Beam, 1995), the time constant of activation (τ_{act}) was determined by fitting a single exponential function to the peak current. Typical fits are illustrated in Fig. 5 (*left*) for SkC15 and for mutations that slowed (R168Q) or accelerated (R171E) activation. All of the S4 mutations in repeats I and III significantly altered τ_{act}, whereas the S4 mutations in repeats II and IV did not have a significant effect (Fig. 5, *top right*). This pattern was very similar to that observed for the repeat dependence of the effects of S4 mutations on $V_{1/2}$ (Fig. 3, *middle*). In the heptad repeat motif, the L182V mutation caused a slowing of activation, and the other mutations were without effect (Fig. 5, *bottom right*).

The effects of the S4 mutations on τ_{act} provide further support for the idea that repeats I and III have a more prominent role in activation than repeats II and IV. Furthermore, the effects of both the S4 and heptad repeat mutations suggest that independent mechanisms might govern the voltage dependence and kinetics of activation. Thus three mutations had a large effect on $V_{1/2}$ but no significant effect on τ_{act} (L196V, L1045V, and I1059V), and one mutation had no significant effect on $V_{1/2}$, but caused the largest slowing of activation (R168Q). Furthermore, mutation R171Q (single charge reduction) caused a depolarizating shift in $V_{1/2}$ and slowed activation, whereas R171E (double charge reduction) caused an even larger depolarizing shift, but unexpectedly had the opposite effect of speeding activation.

DISCUSSION

We have characterized the effects of mutations in S4 segments and in the heptad repeat motif on the voltage dependence ($V_{1/2}$, z_g) and kinetics of activation of an L-type calcium channel. We found that single R→Q mutations in the S4 segments of repeats I and III shift $V_{1/2}$, decrease z_g, and increase τ_{act}, whereas the comparable mutations in repeats II and IV do not significantly affect $V_{1/2}$ or τ_{act} and have a relatively small effect on z_g. Charge-conserving mutations (L/I→V) of the heptad motif region in repeats I and III had variable effects on z_g and τ_{act}. A consistent, positive shift in $V_{1/2}$ was produced by mutations closer to S4 and a consistent negative shift by mutations closer to S5.

The physical interpretation of alterations in activation depends on the model used to describe channel gating. If the channel is approximated as having only two states (closed and open), then the fraction of open channels is given by

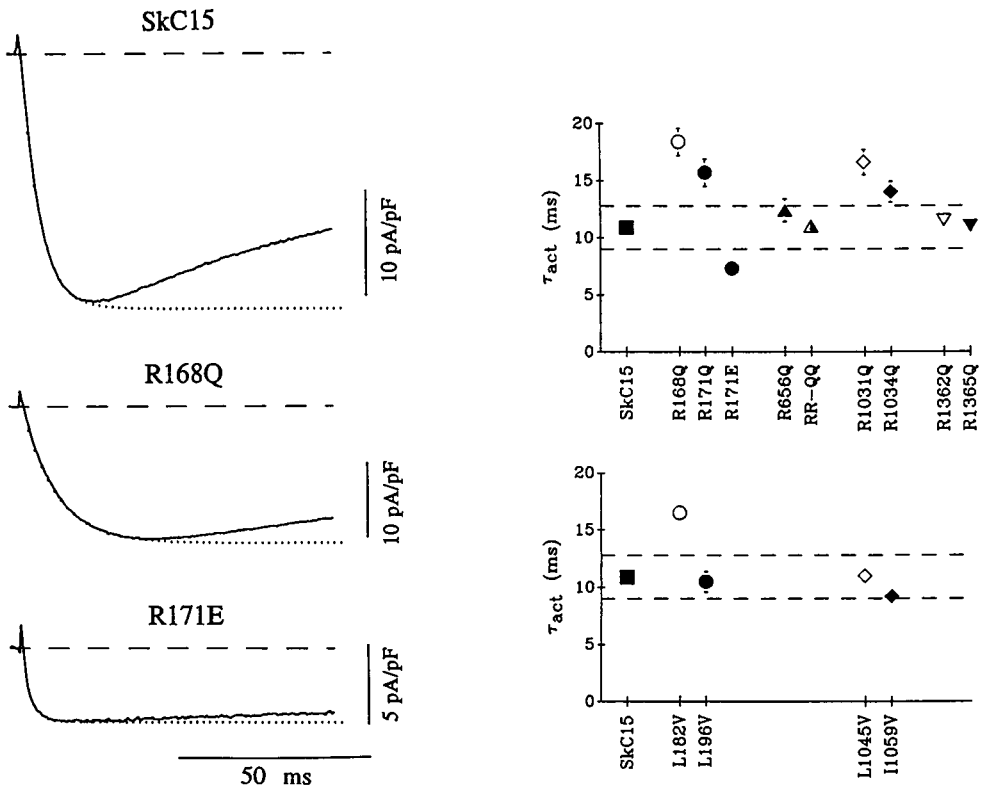

FIGURE 5 Time constant of current activation (τ_{act}) for SkC15 and its mutants. (*Left*) To obtain τ_{act}, a single exponential function (*dotted line*) was fitted to the current at the potential that elicited the maximum current for a 200-ms test pulse (Tanabe et al., 1991). Representative currents are shown for SkC15 (20 mV); R168Q (20 mV), which resulted in the slowest activation; and R171E (40 mV), which resulted in the fastest activation. (*Right, top*) Average values of τ_{act} for S4 mutants. τ_{act} was significantly affected only by mutations in repeats I and III and was decreased only by R171E. (*Right, bottom*) Average values of τ_{act} heptad motif mutations. Only L182V had a significant effect.

(Hille, 1992)

$$\frac{O}{O+C} = \frac{1}{1+\exp[(w - z_g eV)/k_B T]}, \qquad z_g = \sum z_i d_i \qquad (2)$$

where w is the conformational energy difference between the closed (C) and open (O) states in the absence of a membrane field; z_g is the effective gating charge, which is the sum of the individual charges that move (z_i) times the fraction of the membrane field traversed (d_i); e is the electron charge; V the transmembrane potential; k_B is Boltzmann's constant; and T is the absolute temperature. With this model, a decrease in either z_i or d_i would decrease steepness and cause a rightward shift of the midpoint potential (i.e., the voltage at which $z_g eV = w$). By contrast, a change in w would affect only $V_{1/2}$. That one S4 mutation (R1034Q) decreased z_g and caused a leftward shift of $V_{1/2}$ suggests that S4 mutations can affect both z_g and w.

If all of the S4 positive residues in each of the four repeats contributed equally to gating charge, then z_g should decrease linearly with charge reduction. In our experiments we found that the R171 mutations approximately satisfy this prediction. However, many other mutations did not meet this expectation, such as R656Q and R653Q-R656Q. Therefore, a simple charge reduction is insufficient to explain the effects of the S4 mutations on z_g. In terms of the two-state model (Eq. 1), the charge-conserving mutations in the heptad motif would be interpreted as altering both w and d, because these mutations changed both $V_{1/2}$ and z_g.

An alternative to the two-state model would be to assume that the independent movement of voltage sensors in all four repeats is required for the calcium channel to open. With a model of independent sensors, inferences about voltage sensor movement in the different repeats can be drawn from the mutation-induced shifts in $V_{1/2}$. Specifically, changes in the voltage dependence of channel opening will only be seen for voltage sensors that move (in either SkC15 or its mutants) over a range of potentials close to that at which channels open. For example, shifting the potential dependence of a single voltage sensor's movement would not affect $V_{1/2}$ for channel opening if that sensor moved at considerably more negative potentials than the other three sensors. In contrast, shifting the voltage dependence of a sensor that moved at more positive potentials than the other three sensors would necesarily cause a change in $V_{1/2}$. We found that three mutations caused a negative shift of $V_{1/2}$ (Table 1). These mutations were in repeat I (L196V) or repeat III (R1034Q and I1059V). This suggests that voltage sensors in repeats I and III move over potentials close to those causing channel opening. Moreover, the observation that S4 mutations in repeats II and IV had no effect on $V_{1/2}$

suggests that voltage sensors in these two repeats move at potentials more negative than those causing movement of voltage sensors in repeats I and III. Consistent with the idea that movement of sensors in repeats I and III has a voltage dependence closer to that of channel opening, and rightward shifted compared to voltage sensor movements in repeats II and IV, only S4 mutations in repeats I and III affected the time constant of activation. Of course, it is also possible that the S4 mutations we tested in repeats II and IV had no effect on the voltage sensors in those repeats, or that changes we observed in channel activation reflect altered interactions between repeats rather than altered behavior of single repeats.

Substitutions in the heptad motif of the SkC15 calcium channel caused shifts in $V_{1/2}$ in the same direction as the equivalent mutations in the *Shaker* potassium channel (McCormack et al., 1991) (see Table 1). The parallelism between the direction of shifts and position within the heptad motif exists not only between the *Shaker* channel and the calcium channel as described here, but also between the *Shaker* channel and the heptad motif of a rat brain sodium channel. Specifically, the L860F mutation in repeat II of the rat brain IIa sodium channel causes a depolarizing shift, just as the equivalent *Shaker* leucine mutation does (Auld et al., 1990). Taken together, these results suggest that the heptad motif plays a similar, fundamental role in the activation of distantly related, voltage-gated channels. The close association of the heptad motif with the S4 segment and its charged amino acids suggests that these two regions work together to couple channel activation to membrane depolarization.

We thank Kim Lopez and Robin Morris for their excellent technical assistance.

This work was supported by the National Institutes of Health (NS 24444 to KGB) and the Muscular Dystrophy Association (to JG).

REFERENCES

Adams, B. A., and K. B. Beam. 1989. A novel calcium current in dysgenic skeletal muscle. *J. Gen. Physiol.* 94:429–444.

Adams, B. A., T. Tanabe, A. Mikami, S. Numa, and K. G. Beam. 1990. Intramembrane charge movement restored in dysgenic skeletal muscle by injection of dihydropyridine receptor cDNAs. *Nature.* 346:569–572.

Auld, V. J., A. L. Goldin, D. S. Krafte, W. A. Catterall, H. A. Lester, N. Davidson, and R. J. Dunn. 1990. A neutral amino acid change in segment IIS4 dramatically alters the gating properties of the voltage-dependent sodium channel. *Proc. Natl. Acad. Sci. USA.* 87:323–327.

Chen, L.-Q., V. Santarelli, R. Horn, and R. G. Kallen. 1996. A unique role for the S4 segment of domain 4 in the inactivation of sodium channels. *J. Gen. Physiol.* 108:549–556.

Dirksen, R. T., and K. G. Beam. 1995. Single calcium channel behavior in native skeletal muscle. *J. Gen. Physiol.* 105:227–247.

Dirksen, R. T., and K. G. Beam. 1996. Unitary behavior of skeletal, cardiac, and chimeric L-type Ca^{2+} channels expressed in dysgenic myotubes. *J. Gen. Physiol.* 107:731–742.

García, J., T. Tanabe, and K. G. Beam. 1994. Relationship of calcium transients to calcium currents and charge movements in myotubes expressing skeletal and cardiac dihydropyridine receptors. *J. Gen. Physiol.* 103:125–147.

George, A. L., J. Komisarof, R. G. Kallen, and R. L. Barchi. 1992. Primary structure of the adult human skeletal muscle voltage-dependent Na^+ channel. *Ann. Neurol.* 31:131–137.

Hamill, O. P., A. Marty, E. Neher, B. Sakmann, and F. J. Sigworth. 1981. Improved patch-clamp techniques for high-resolution current recording from cells and cell-free membrane patches. *Pflügers Arch.* 391:85–100.

Hille, B. 1992. Ionic Channels of Excitable Membranes. Sinauer Associates, Sunderland, MA. 440–444.

Holmgren, M., M. E. Jurman, and G. Yellen. 1996. N-type inactivation and the S4–S5 region of the Shaker K^+ channel. *J. Gen. Physiol.* 108: 195–206.

Isacoff, E. Y., Y. N. Jan, and L. Y. Jan. 1991. Putative receptor for the cytoplasmic inactivation gate in the *Shaker* K^+ channel. *Nature.* 353: 86–90.

Jurman, M. E., L. M. Boland, Y. Liu, and G. Yellen. 1994. Visual identification of individual transfected cells for electrophysiology using antibody-coated beads. *Biotechniques.* 17:876–880.

Larsson, H. P., O. S. Baker, D. S. Dhillon, and E. Y. Isacoff. 1996. Transmembrane movement of the *Shaker* K^+ channel S4. *Neuron.* 16:387–397.

Liman, E. R., P. Hess, F. Weaver, and G. Koren, G. 1991. Voltage-sensing residues in the S4 region of a mammalian K^+ channel. *Nature.* 353: 752–756.

Logothetis, D. E., S. Movahedi, C. Satler, K. Lindpaintner, and B. Nadal-Ginard. 1992. Incremental reductions of positive charge within the S4 region of a voltage-gated K± channel result in corresponding decreases in gating charge. *Neuron.* 8:531–540.

Lopez, G. A., Y. N. Jan, and L. Y. Jan. 1991. Hydrophobic substitution mutations in the S4 sequence alter voltage-dependent gating in *Shaker* K^+ channels. *Neuron.* 7:327–336.

MacKinnon, R. 1991. Determination of the subunit stoichiometry of a voltage-activated potassium channel. *Nature.* 350:232–235.

Mannuzzu, L. M., M. M. Moronne, and E. Y. Isacoff. 1996. Direct physical measure of conformational rearrangement underlying potassium channel gating. *Science.* 271:213–216.

McCormack, K., M. A. Tanouye, L. E. Iverson, J.-W. Lin, M. Ramaswami, T. McCormack, J. T. Campanelli, M. K. Mathew, and B. Rudy. 1991. A role for hydrophobic residues in the voltage-dependent gating of Shaker K^+ channels. *Proc. Natl. Acad. Sci. USA.* 88:2931–2935.

Mikami, A., K. Imoto, T. Tanabe, T. Niidome, Y. Mori, H. Takeshima, S. Narumiya, and S. Numa. 1989. Primary structure and functional expression of the cardiac dihydropyridine-sensitive calcium channel. *Nature.* 340:230–233.

Mori, Y., T. Friedrich, M.-S. Kim, A. Mikami, J. Nakai, P. Ruth, E. Bosse, F. Hofmann, V. Flockerzi, T. Furuichi, K. Mikoshiba, K. Imoto, T. Tanabe, and S. Numa. 1991. Primary structure and functional expression from complementary DNA of a brain calcium channel. *Nature.* 350: 398–402.

Noda, M., T. Ikeda, T. Kayano, H. Suzuki, H. Takeshima, M. Kurasaki, H. Takahashi, H., and S. Numa. 1986. Existence of distinct sodium channel messenger RNAs in rat brain. *Nature.* 320:188–192.

Papazian, D. M., X. M. Shao, S.-A. Seoh, A. F. Mock, Y. Huang, and D. H. Wainstock. 1995. Electrostatic interactions of S4 voltage sensor in Shaker K^+ channel. *Neuron.* 14:1293–1301.

Papazian, D. M., L. C. Timpe, Y. N. Jan, and L. Y. Jan. 1991. Alteration of voltage-dependence of *Shaker* potassium channel by mutations in the S4 sequence. *Nature.* 349:305–310.

Sanger, F., S. Nicklen, and A. R. Coulson. 1977. DNA sequencing with chain-termination inhibitors. *Proc. Natl. Acad. Sci. USA.* 74:5463–5467.

Sayers, J. R., and F. Eckstein. 1989. Site-directed mutagenesis, based on the phosphorotioate approach. *In* Protein Function: A Practical Approach. T. E. Creighton, editor. IRL Press, New York. 279–295.

Schwarz, T. L., B. L. Tempel, D. M. Papazian, Y. N. Jan, and L. Y. Jan. 1988. Multiple potassium channel components are produced by alternative splicing at the *Shaker* locus in *Drosophila. Nature.* 331:137–143.

Sigworth, F. J. 1993. Voltage gating of ion channels. *Q. Rev. Biophys.* 27:1–40.

Silver, J., T. Limjoco, and S. Feinstone. 1995. Site-specifiic mutagenesis using the polymerase chain reaction. *In* PCR Strategies. M. A. Innis, D. H. Gelfand, and J. J. Sninsky, editors. Academic Press, San Diego, CA. 179–188.

Stühmer, W., F. Conti, H. Suzuki, X. Wang, M. Noda, N. Yahagi, H. Kubo, and S. Numa. 1989. Structural parts involved in activation and inactivation of the sodium channel. *Nature.* 339:597–603.

Tanabe, T., B. A. Adams, S. Numa, and K. G. Beam. 1991. Repeat I of the dihydropyridine receptor is critical in determining calcium channel activation kinetics. *Nature.* 352:800–803.

Tanabe, T., K. G. Beam, J. A. Powell, and S. Numa. 1988. Restoration of excitation-contraction coupling and slow calcium current in dysgenic muscle by dihydropyridine receptor complementary DNA. *Nature.* 336: 134–139.

Tanabe, T., H. Takeshima, A. Mikami, V. Flockerzi, H. Takahashi, K. Kangawa, M. Kojima, H. Matsuo, T. Hirose, and S. Numa. 1987. Primary structure of the receptor for calcium channel blockers from skeletal muscle. *Nature.* 328:313–318.

Tempel, B. L., D. M. Papazian, T. L. Schwarz, Y.-N. Jan, and L. Y. Jan. 1987. Sequence of a probable potassium channel component encoded at *Shaker* locus of *Drosophila. Science.* 237:770–775.

Tytgat, J., K. Nakazawa, A. Gross, and P. Hess. 1993. Pursuing the voltage sensor of a voltage-gated mammalian potassium channel. *J. Biol. Chem.* 268:23777–23779.

Yang, N., A. L. George, and R. Horn. 1996. Molecular basis of charge movement in voltage-gated sodium channels. *Neuron.* 16:113–122.

Yang, N., and R. Horn. 1995. Evidence for voltage-dependent S4 movement in sodium channels. *Neuron.* 15:213–218.